PRAMANA
— journal of
physics

Vol. 84, No. 6
June 2015
pp. 1033–1040

A model for the direct-to-indirect band-gap transition in monolayer $MoSe_2$ under strain

RUMA DAS and PRIYA MAHADEVAN*

Department of Condensed Matter Physics and Material Science, S.N. Bose National Centre for Basic Sciences, Kolkata 700 098, India

*Corresponding author. E-mail: priya@bose.res.in

DOI: 10.1007/s12043-015-0996-6; ***e*Publication:** 28 May 2015

Abstract. A monolayer of $MoSe_2$ is found to be a direct band-gap semiconductor. We show, within *ab-initio* electronic structure calculations, that a modest biaxial tensile strain of 3% can drive it into an indirect band-gap semiconductor with the valence band maximum (VBM) shifting from K point to Γ point. An analysis of the charge density reveals that while Mo–Mo interactions contribute to the VBM at 0% strain, Mo–Se interactions contribute to the highest occupied band at Γ point. A scaling of the hopping interaction strengths within an appropriate tight binding model can capture the transition.

Keywords. Biaxial tensile strain; tight binding model; layered transition metal dichalcogenide; *ab-initio*.

PACS Nos 73.22.−f; 71.20.Nr

1. Introduction

Layered transition metal sulphides and selenides have been widely studied since the 1960s for wide-ranging applications which include their use as a dry lubricant [1], in catalysis [2], photovoltaics [3] as well as batteries [4]. The recent interest in graphene [5–7] has brought the focus onto these materials which have the advantage of being semiconducting in addition to being layered. Interestingly, in each of these materials, while the single layer is a direct band-gap material [8,9], the bilayer and beyond become indirect band-gap materials [9,10]. Indirect band-gap materials are suitable for various applications such as photovoltaics [3] where one would like to bring about the spatial separation of the generated electron–hole pair. Considering a monolayer of MoS_2, we showed that a modest strain of 2% [11] was sufficient to bring about the transition from a direct band-gap semiconductor to an indirect band-gap one. Analysing the charge density in the unstrained case, it was found that the valence band maximum (VBM) which was at K point was contributed by Mo d–Mo d interactions, while the highest occupied band at Γ point is contributed by Mo d–S p interactions. Under strain, one changed the Mo–Mo

distances while keeping the Mo–S separation almost unchanged. As the hopping interaction strengths for electrons on orbitals with angular momenta l and l' respectively vary as $1/r^{l+l'+1}$ according to an empirical law referred to as to Harrison's scaling law [12], it was shown that a scaling of the hopping interaction strengths with distance could explain the direct-to-indirect band-gap transition.

In this work, we extend the model to another layered transition metal dichalcogenide, $MoSe_2$. The unstrained band structure for this system calculated within *ab-initio* electronic structure calculations is found to reproduce the experimental observation [13] that this system is a direct band-gap semiconductor. The VBM is at K point and the conduction band bottom (CBM) is also at K point. A biaxial strain of 3% in the case of $MoSe_2$ is able to bring about a change-over with the band at Γ point becoming the VBM. We then have a transition from a direct band-gap material to an indirect band-gap one. In order to model this transition, a tight-binding model has been set up for the system. The onsite energies as well as the hopping interaction strengths have been estimated by fitting the *ab-initio* band structure for the unstrained case. The transition metal d–transition metal d interaction strengths are allowed to vary with distance according to Harrison's scaling law [12]. This model can capture the strain-induced direct-to-indirect band-gap transition.

2. Methodology

The electronic structure of the monolayer $MoSe_2$ has been calculated within a plane-wave projected augmented wave implementation of density functional theory using the VASP [14] code. In the case of $MoSe_2$ the experimental crystal structure [13] has been taken. A vacuum of 20 Å was used between successive monolayers to minimize interactions between images in the periodic supercell method that we use for this structure. While the lattice parameters were kept fixed at the experimental values, the internal positions were optimized in each case. Projected augmented wave [15] potentials were used to solve the electronic structure self-consistently using a K-point mesh of $12\times12\times1$. PBE [16] potentials were used for the exchange correlation functionals and the calculations were performed as a function of biaxial tensile strain.

In order to determine appropriate basis for the tight-binding model, the Mo and Se partial density-of-states are shown in figure 1. The zero of energy in figure 1 is the Fermi energy. One finds that the Mo d states contribute in the energy window 5 eV below the Fermi energy and upto 5 eV above the Fermi energy. The Mo s and Mo p states are more extended and so their weight in any given energy window is low. However, our earlier work had shown that to get a good description of the *ab-initio* band structure in a wide energy window from 10 eV below the Fermi level to around 5 eV above, one needs to include the Mo s p d states in the basis. The Se s states are around 12 eV below the Fermi level, with Se p states contributing dominantly in the region of interest. Se d states are found to contribute in the energy window beyond 5 eV above the Fermi level. We therefore include Se s, p, d states in the basis for the tight-binding model considered.

The tight-binding parameters were determined by a least-square error minimization [17]. For the strained case, a Harrison's-type scaling [12] of the hopping integrals of the form $1/r^{l+l'+1}$ has been assumed for the Mo d–Mo d interaction for deviations upto 0.1 Å

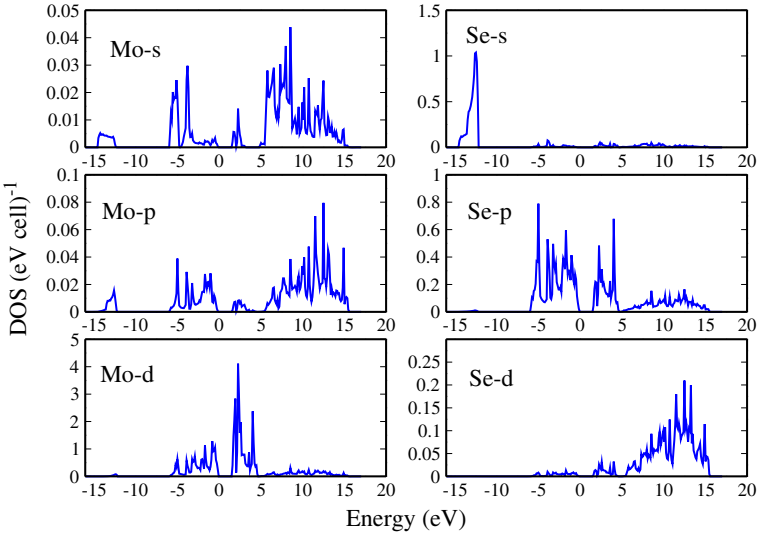

Figure 1. The atom and angular momentum projected partial density-of-states for Mo and Se atoms from *ab-initio* calculations using GGA potentials at 0% strain. The zero of energy corresponds to the valence band maximum.

about the distance at which the hopping interaction strength is defined, while the onsite energies were allowed to vary.

3. Results and discussion

The structure of the monolayer $MoSe_2$ is shown in figure 2. The Mo–Mo distance at the experimental lattice constant which has been considered here is 3.25 Å. Under 3% biaxial tensile strain, Mo–Mo and Se–Se distances are found to become 3.35 Å. The Mo–Se distance however remains unchanged. The *ab-initio* band dispersions for $MoSe_2$ plotted

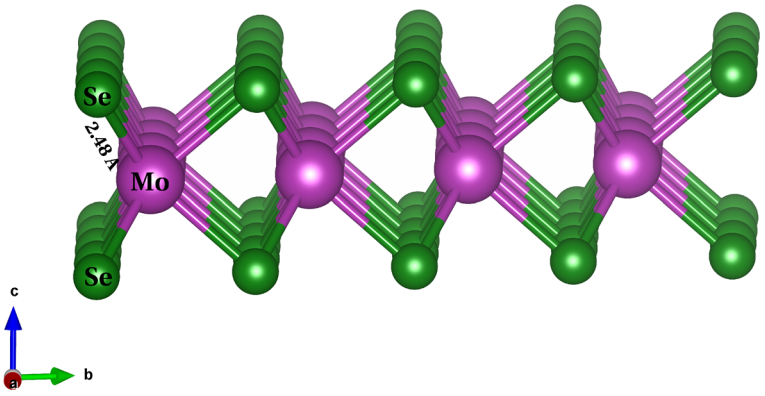

Figure 2. Crystal structure of a monolayer of $MoSe_2$.

along various symmetry directions are shown in figure 3. The calculations capture the semiconducting nature of the compound and a band gap of 1.59 eV is found at 0% strain. This is in reasonable agreement with the experimental value of 1.55 eV [13]. While LDA/GGA calculations are usually found to underestimate the band gap, the agreement is fortuitious.

The *ab-initio* band structure is fit to a tight-binding model discussed in §2. The parameters entering the tight-binding Hamiltonian are determined by a least-square-error minimization process. All bands were not considered in this fitting except all the bands comprising the valence band in the energy window −7 eV to the Fermi energy as well as two bands comprising the conduction band. The *ab-initio* band structure is shown in black solid line while the tight-binding band structure is shown in red dashed line in the same figure. The description in this minimal tight-binding model is reasonable. The parameters entering the tight-binding Hamiltonian are given in table 1. The onsite energies are denoted by E_s where the subscript corresponds to the orbital involved. For the Mo d orbitals we found the need to allow for the degeneracy lifting of the d orbitals. The intersite hopping interactions have been parametrized in terms of the Slater Koster parameters and are tabulated for the first neighbour Mo–Se sites as well as second neighbour Mo–Mo and Se–Se sites.

In order to understand the nature of interactions contributing to the VBM at 0% strain, we have plotted the charge density in figure 4 corresponding to the eigenvalue at K point. One finds substantial interaction between the in-plane d orbitals – d_{xy} and $d_{x^2-y^2}$ contributing to the eigenvalue corresponding to the VBM arising from the extended nature

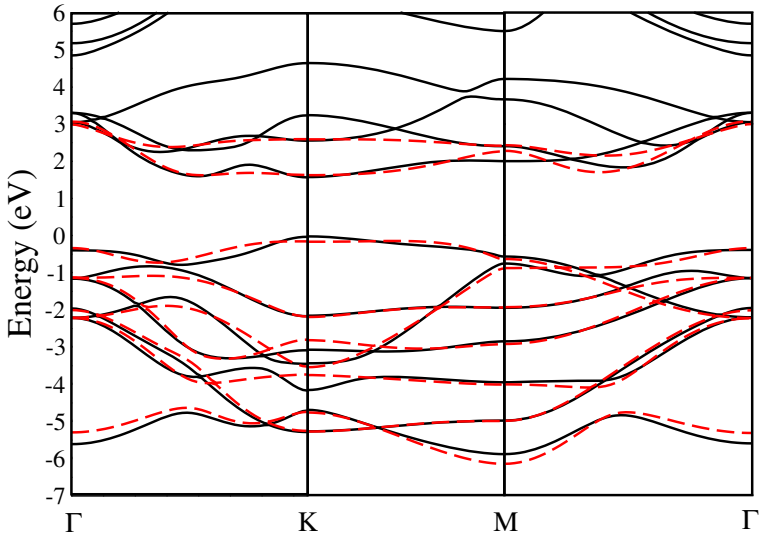

Figure 3. Comparison of *ab-initio* band dispersions (solid line) for the monolayer $MoSe_2$ at its experimental lattice constant (0% biaxial tensile strain), using GGA potentials and the fitted tight-binding bands (dashed line), using a basis consisting of Mo s, p, d and Se s, p, d states. The zero of energy corresponds to the valence band maximum.

Table 1. Parameters obtained from least-squared-error fitting of the *ab-initio* band structure onto a tight-binding model using s, p, d orbitals of Mo and Se for the monolayer $MoSe_2$ at 0% biaxial tensile strain. The energies are in eV.

	E_s	E_p	$E_{d_{xy}}$	$E_{d_{yz}}$	$E_{d_{zx}}$	$E_{d_{x^2-y^2}}$	$E_{d_{z^2}}$
Mo	4.88	8.38	3.76	1.80	1.80	3.76	1.08
Se	−14.55	−4.12	8.45	8.45	8.45	8.45	8.45
	E(Mo,Mo)	E(Mo,S)	E(S,S)				
$ss\sigma$	−00.820	−01.032	−00.200				
$sp\sigma$	00.690	01.842	00.050				
$sd\sigma$	−00.010	−00.715	−00.152				
$pp\sigma$	01.340	01.431	00.973				
$pp\pi$	−00.550	−00.192	−00.132				
$pd\sigma$	−01.290	−01.490	00.000				
$pd\pi$	00.290	03.011	00.490				
$dd\sigma$	00.540	−03.863	−00.005				
$dd\pi$	00.041	02.308	00.143				
$dd\delta$	−00.001	−00.390	−00.002				
$ps\sigma$	−00.690	−01.196	−00.050				
$ds\sigma$	−00.010	−01.658	−00.152				
$dp\sigma$	01.290	02.560	00.000				
$dp\pi$	−00.290	−00.384	−00.490				

of the wave function of the 4d transition metal atom. So, even if separations are as large as 3.25 Å, there is significant interaction. On the other hand, the highest occupied band at Γ point is contributed by Mo d–Se p interactions involving d_{z^2} orbitals on Mo and p_z orbitals on Se which is shown in figure 5. When we apply biaxial strain, one finds that the Mo–Se bond length does not change, while the Mo– Mo bond is elongated. This immediately suggests a route to modify the character of the VBM via the strain. The Mo d–Mo d interactions can be modified when the Mo–Mo separation is increased. The hopping

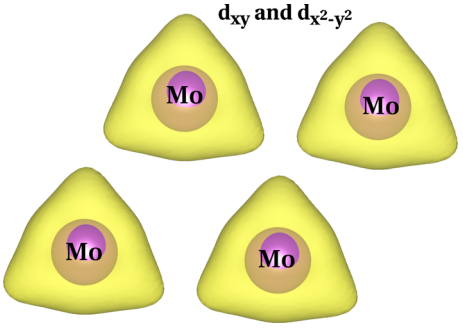

Figure 4. The charge density plot for the monolayer $MoSe_2$ for the highest occupied band at K point obtained from *ab-initio* calculations using GGA potentials at 0% strain.

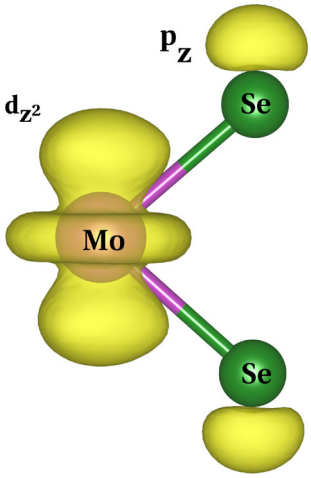

Figure 5. The charge density plot for the monolayer $MoSe_2$ for the highest occupied band at Γ point obtained from *ab-initio* calculations using GGA potentials at 0% strain.

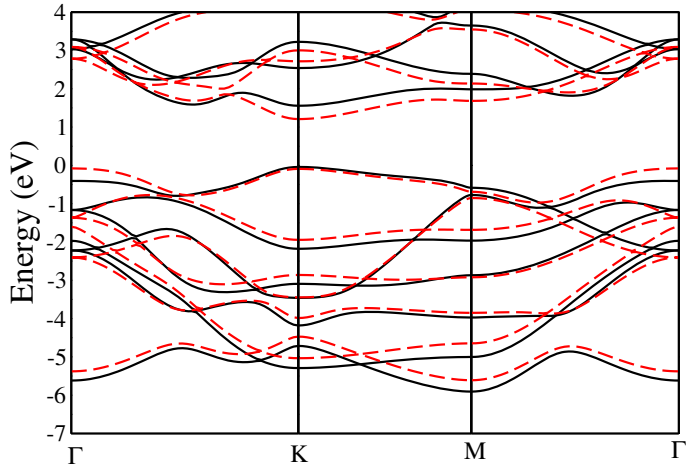

Figure 6. Comparison of *ab-initio* band dispersions for the monolayer $MoSe_2$ at its experimental lattice constant at 0% biaxial tensile strain (solid line) and 3% biaxial tensile strain (dashed line) using GGA potentials. The zero of energy corresponds to the valence band maximum.

interactions between two orbitals scale inversely with distance according to a power law. Increasing the separation decreases the interaction strength. As the VBM is contributed by antibonding states arising from Mo–Mo interactions, one finds that these states move deeper into the valence band. Indeed when we plot the band structure under 3% strain, we find a cross-over of the VBM from K to Γ in figure 6. In the figure, we superpose the *ab-initio* band dispersions calculated at 0% strain as well as 3% strain. As under

Table 2. The onsite energies obtained from least-squared-error fitting of the *ab-initio* band structure onto a tight-binding model using *s*, *p*, *d* orbitals of Mo and Se for the monolayer $MoSe_2$ at 3% biaxial tensile strain. The energies are in eV.

	E_s	E_p	$E_{d_{xy}}$	$E_{d_{yz}}$	$E_{d_{zx}}$	$E_{d_{x^2-y^2}}$	$E_{d_{z^2}}$
Mo	5.23	8.78	4.26	1.99	1.99	4.26	1.54
Se	−14.78	−4.36	6.37	6.37	6.37	6.37	6.37

strain, only the second neighbour interaction strengths are affected, one does not expect too much change in band structure with strain. While, there seems large differences at first sight, shifting the dominantly Se *p* states in the 3% strain calculation are found to match up with the bands at 0% strain calculation. Similarly, we can shift the bands contributed dominantly by Mo *d* states in the 3% calculation to those in the unstrained case. This indicates that large differences emerge from charge transfer between the Mo and Se sites.

In order to determine the parameters entering the tight-binding Hamiltonian at 3% strain, we used the extracted parameters at 0% strain. The onsite energies were allowed to vary, while the hopping interaction strengths were kept fixed at the values of table 1 and were allowed to scale according to Harrison's scaling law [12] discussed earlier. The values of onsite energies extracted from the fitting are listed in table 2. The scaling affected the Se–Se as well as Mo–Mo interaction strengths. A comparison of the

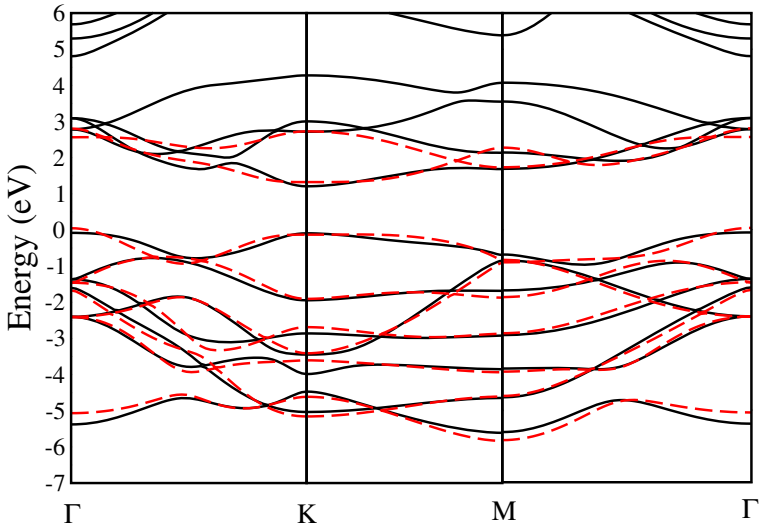

Figure 7. Comparison of *ab-initio* band dispersions (solid line) for the monolayer $MoSe_2$ at its experimental lattice constant (3% biaxial tensile strain), using GGA potentials and the fitted tight-binding bands (dashed line), using a basis consisting of Mo *s*, *p*, *d* and Se *s*, *p*, *d* states. The zero of energy corresponds to the valence band maximum.

ab-initio band structure and the best-fit tight-binding band structure are shown in figure 7. The tight-binding model can capture the transition from direct into an indirect band-gap semiconductor and the valence band maximum is shifted to Γ point.

4. Conclusion

In conclusion, we have set up a realistic tight-binding model to discuss the electronic structure of $MoSe_2$ under strain. The model can capture the direct-to-indirect band-gap transition with strain.

Acknowledgements

The authors thank the Department of Science and Technology (DST) India, Nanomission for funding through an individual project, the Thematic Unit of Excellence on Computational Materials Science (TUE-comp) as well as the Unit of Nanoscience and Nanotechnology (UNANST). RD thanks the Council of Scientific and Industrial Research (CSIR), India.

References

[1] K H Hu, X G Hu and X J Sun, *Appl. Surf. Sci.* **256**, 2517 (2010)
[2] W K Ho, J C Yu, J Lin, J G Yu and P S Li, *Langmuir* **20**, 5865 (2004)
[3] E Fortin and W Sears, *J. Phys. Chem. Solids* **43**, 881 (1982)
[4] C Feng, J Ma, H Li, R Zeng, Z Guo and H Liu, *Mater. Res. Bull.* **44**, 1811 (2009)
[5] K S Novoselov, A K Geim, S V Morozov, D Jiang, Y Zhang, S V Dubonos, I V Grigorieva and A A Firsov, *Science* **306**, 666 (2004)
[6] A H C Neto, F Guinea, N M R Peres, K S Novoselov and A K Geim, *Rev. Mod. Phys.* **81**, 109 (2009)
[7] Y Wu, Y-M Lin, A A Bol, K A Jenkins, F Xia, D B Farmer, Y Zhu and P Avouris, *Nature* **472**, 74 (2011)
[8] C Lee, H Yan, L E Brus, T F Heinz, J Hone and S Ryu, *ACS Nano* **4**, 2695 (2010)
[9] A D Yoffe, *Annu. Rev. Mater. Sci.* **3**, 147 (1973)
[10] G L Frey, S Elani, M Homyonfer, Y Feldman and R Tenne, *Phys. Rev. B* **57**, 6666 (1998)
[11] R Das, B Rakshit, S Debnath and P Mahadevan, *Phys. Rev. B* **89**, 115201 (2014)
[12] W A Harrison, *Electronic structure and the properties of solids: The physics of the chemical bond* (Dover, New York, USA, 1967)
[13] S Tongay, J Zhou, C Ataca, K Lo, T S Matthews, J Li, J C Grossman and J Wu, *Nano Lett.* **12**, 5576 (2012)
[14] G Kresse and J Furthmüller, *Phys. Rev. B* **54**, 11169 (1996)
[15] G Kresse and D Joubert, *Phys. Rev. B* **59**, 1758 (1999)
[16] J Paier, R Hirschl, M Marsman and G Kresse, *J. Chem. Phys.* **122**, 234102 (2005)
[17] P Mahadevan, N Shanthi and D D Sarma, *Phys. Rev. B* **54**, 11, 199 (1996)